

## 23.5 Optical Interconnect Technologies for High-Speed VLSI Chips Using Silicon Nano-Photonics

Keishi Ohashi<sup>1</sup>, Junichi Fujikata<sup>1</sup>, Masafumi Nakada<sup>1</sup>, Tsutomu Ishi<sup>1</sup>, Kenichi Nishi<sup>1</sup>, Hirohito Yamada<sup>1</sup>, Muneo Fukaiishi<sup>2</sup>, Masayuki Mizuno<sup>2</sup>, Koichi Nose<sup>2</sup>, Ichiro Ogura<sup>3</sup>, Yutaka Urino<sup>1</sup>, Toshio Baba<sup>1</sup>

<sup>1</sup>NEC, Tsukuba, Japan

<sup>2</sup>NEC, Sagamihara, Japan

<sup>3</sup>NEC, Kawasaki, Japan

Optical interconnects offer several advantages, including low power loss, small cross-talk, and no electromagnetic interference (EMI), over transmission lines at frequencies >10GHz. These advantages open up potential on-chip applications of optics [1] such as global optical wiring and optical clock distribution, as shown in Fig. 23.5.1. Due to recent progress in optical waveguide technologies, optical wiring between chips is becoming increasingly realistic, but optical wiring within a chip is still viewed with some skepticism. One reason for this is the absence of high-performance  $\mu\text{m}$ -size optoelectronic (OE) and electrooptic (EO) elements suitable for CMOS process technologies. To address this challenge, new approaches are presented for integrating OE and EO elements on integrated circuit chips.

Direct-gap semiconductors are more widely used for high-speed photodiodes in optical communication than low-cost Si. One of the main reasons for this is that the absorption length of Si is greater than  $10\mu\text{m}$ , resulting in a long carrier drift time and slow response. Here, we demonstrate a "nanophotodiode" that uses a small volume of near-field light to reduce the size of the Si [2, 3]. The device uses a surface-plasmon (SP) antenna to collect light and then creates a small but strong near-field in the Si mesa on the opposite side of the antenna. The size of the Schottky region in the Si mesa can be reduced almost to the size of the near-field region (10-100nm long) and thus the transit time of the carriers is fairly short. The full-width at half-maximum (FWHM) of the impulse response was as fast as  $\sim 20\text{ps}$  even when the bias voltage was less than 1V, as shown in Fig. 23.5.2. The SP antenna acts as a resonant cavity that temporarily reserves optical energy and increases the quantum efficiency (Fig. 23.5.1). Its function as a cavity is similar to that of a Bragg reflector [4] except that the SP antenna creates a small confined near-field through a sub-wavelength aperture. The cavity function makes sense when the resonance is achieved in a shorter time than the response time of the photodiode. It is essential that the near-field area is small to obtain a low junction capacity of  $\sim 10\text{aF}$ . This extremely low capacitance permits the use of high load resistance to obtain a higher output voltage at higher frequencies.

The use of complex back-end amplifiers to switch flip-flops in electronic logic circuits can be avoided by introducing a series of two photodiode circuits illuminated by two different pulse streams with different phases [5]. Combining this transimpedance-amplifier-less (TIA-less) scheme with low-capacitance Si photodiodes gives a promising on-chip OE conversion mechanism. We propose a similar two-photodiode system, but using a single optical clock stream, as shown in Fig. 23.5.3 (Type-A). The response of the Type-A system was simulated by assuming typical 90nm node transistors (channel length  $0.38\mu\text{m}$ ),  $V_{\text{dd}} = 1\text{V}$ , a photodiode with a responsivity of  $0.5\text{A/W}$ , a light power of  $200\text{nW}$  for each photodiode, and a light-pulse duration of  $30\text{ps}$ . A good pulse shape for 5-10GHz clocking can be seen in Fig. 23.5.3. The possible maximum clocking frequency of a Type-A system is 10GHz. We also propose a TIA-less scheme with one photodiode as shown in Fig. 23.5.4 (Type-B). This system has a smaller footprint than that of the Type-A system. Nevertheless, Type-B also

shows a good pulse shape for 5GHz clocking. The possible maximum clocking frequency of Type-B is 7.5GHz. Type-A has fewer transistors resulting in a better frequency response and lower power dissipation. Power consumption in a Type-A photodiode system is  $56\mu\text{W}$  at 5GHz, and  $100\mu\text{W}$  at 10GHz. In the latter case, the total power consumption for the chip and light source is  $100\text{W}$  and  $0.2\text{W}$ , respectively, when the number of the photodiode system is  $10^6$ . Power consumption in a Type-B photodiode system is  $75\mu\text{W}$  at 5GHz. The SP antenna for our first nanophotodiode was about  $10\mu\text{m}$  in diameter, which could be reduced further. The small footprint of the nanophotodiode makes it suitable for optical clock distribution.

The nanophotodiode has a relatively wide bandwidth. The Q-value of the surface plasmon antenna is controlled to between 10 and 50. This makes it suitable for wavelength-division multiplexing (WDM) technology in a chip. Arrayed waveguide gratings (AWGs) based on Si-wires and SiON-wires have been developed. Fig. 23.5.5 shows an eight-channel SiON-AWG (wavelength 770nm to 830nm) designed to couple with Si nanophotodiodes as well as a Si-AWG (wavelength 1520nm to 1580nm) for Ge nanophotodiodes. A combination of Si nanophotodiodes and a SiON AWG could possibly be used for multiple-frequency clocking.

A small ( $\sim 10\mu\text{m}$ ), low-voltage operation EO modulator will be a key technology for (a) an optical on-chip bus, and (b) optical data transmission between chips. The former provides a solution to the problems of using time-division multiplexing (TDM) in an electric on-chip bus. A parallel optical data-communication scheme could be introduced using a simple transfer protocol between multiple blocks. The latter would enable multiple bit transfer between chips through one optical waveguide, which would provide an alternative to electronic serialization/deserialization (SerDes) circuitry. We investigated a Fabry-Perot type on-chip EO modulator with a  $\text{Pb}(\text{Zn},\text{Ti})\text{O}_3$  (PZT) film deposited using an aerosol-deposition (AD) method [6]. The AD PZT film has a high EO coefficient of  $>150\text{pm/V}$ , which is at least one order of magnitude larger than that of conventional films such as lithium niobate ( $\sim 20\text{pm/V}$ ). A Fabry-Perot type EO modulator using AD film has been developed. It is  $10\mu\text{m}$  in size and has an operating voltage of 1V. A Mach-Zehnder-type modulator with a PZT film has also been developed to obtain a wider band nature. Figure 23.5.6 shows that a  $100\mu\text{m}$ -long Mach-Zehnder-type modulator has a sufficient response at 1V. An acceptable transmission property of up to 20GHz was confirmed from the simulated S-parameters of the  $100\mu\text{m}$ -long PZT waveguide.

### Acknowledgments:

The authors would like to thank J. Sone, N. Nishi, S. Sugou, K. Ishihara, K. Kurata, and K. Lister for helpful discussions.

### References:

- [1] D. A. B. Miller et. al., "Opportunities for Optics in Integrated Circuits Applications," *ISSCC Dig. Tech. Papers*, pp. 86-87, Feb., 2005.
- [2] T. Ishi et. al., "Si Nano-Photodiode with a Surface Plasmon Antenna," *Jap. J. Appl. Phys.*, vol. 44, pp. L364-L366, 2005.
- [3] J. Fujikata et. al., "Highly Enhanced Speed and Efficiency of Si Nano-Photodiode with a Surface-Plasmon Antenna," *Extended Abstracts of SSDM 2005*, E-3-3, 2005.
- [4] J. D. Schaub et. al., "Resonant-Cavity-Enhanced High-Speed Si Photodiode Grown by Epitaxial Lateral Overgrowth," *IEEE Photon. Technol. Lett.*, vol. 11, pp. 1647-1649, 1999.
- [5] C. D. Debae et. al., "Receiver-Less Optical Clock Injection for Clock Distribution Networks," *IEEE J. Sel. Top. Quantum Electron.*, vol. 9, no. , pp. 400-409, 2003.
- [6] M. Nakada et. al., "Electro-Optical Properties of  $\text{Pb}(\text{Zr}_{1-x}\text{Ti}_x)\text{O}_3$  ( $x = 0, 0.3, 0.6$ ) Films Prepared by Aerosol Deposition," *Jap. J. Appl. Phys.*, vol. 44, pp. L1088-L1090, 2005.

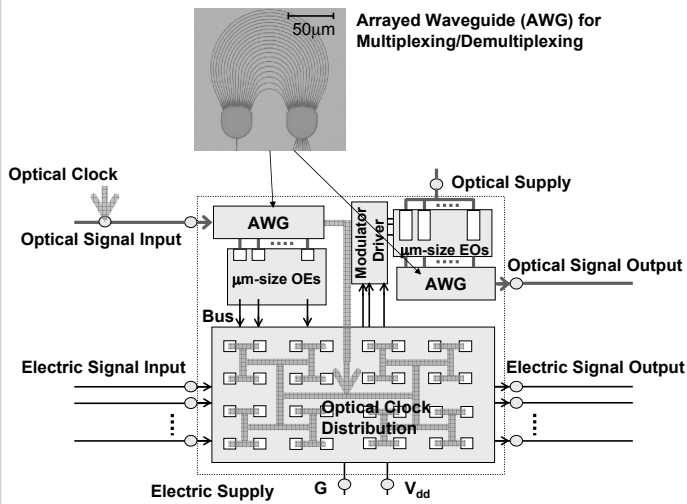


Figure 23.5.1: Schematic concept of Si Nanophotonics.

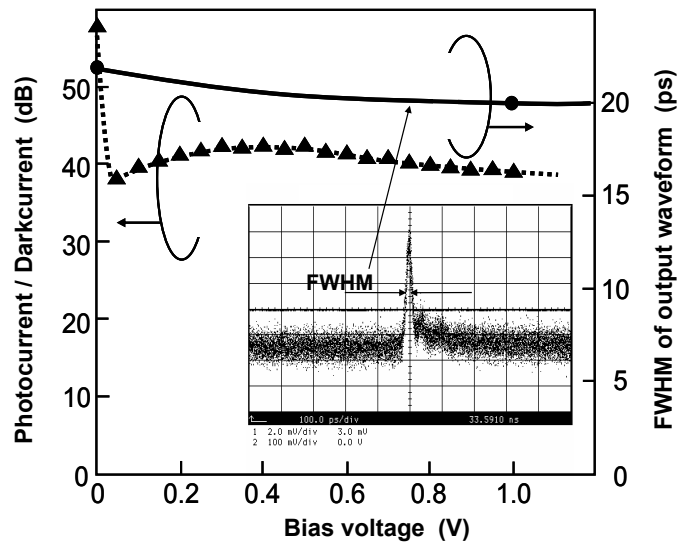


Figure 23.5.2: Pulse response of nanophotodiode.

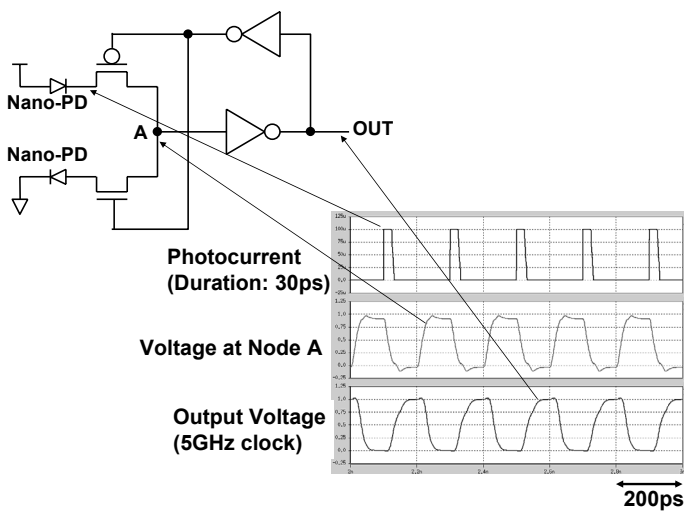


Figure 23.5.3: TIA-less system with two photodiodes (Type-A).

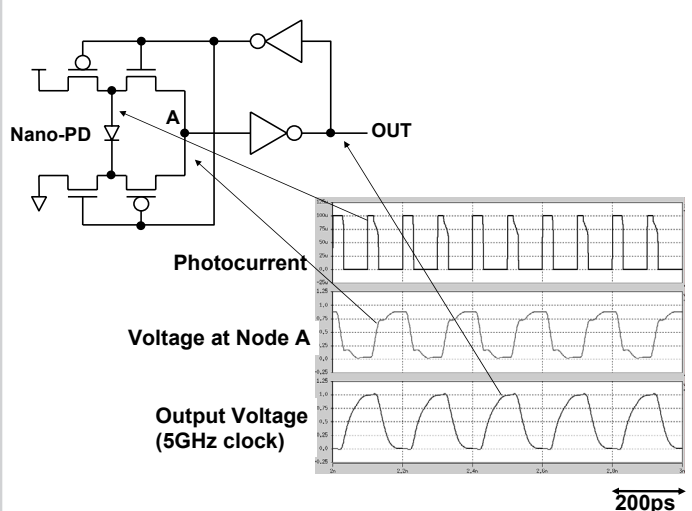


Figure 23.5.4: TIA-less system with one photodiode (Type-B).

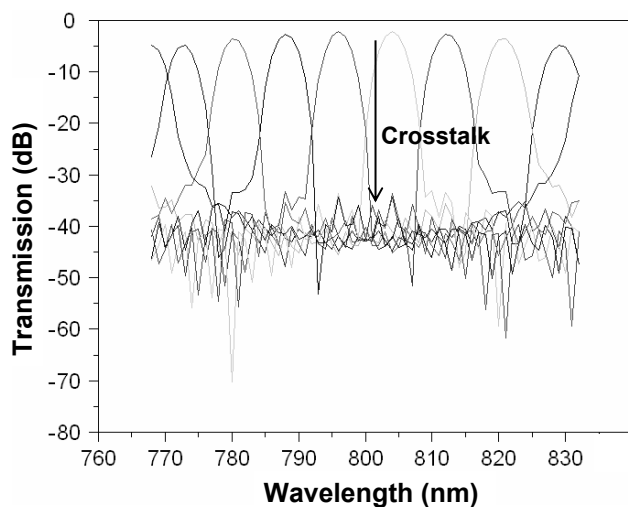


Figure 23.5.5: Simulated demultiplexing characteristics of eight-channel micro SiON-AWG.

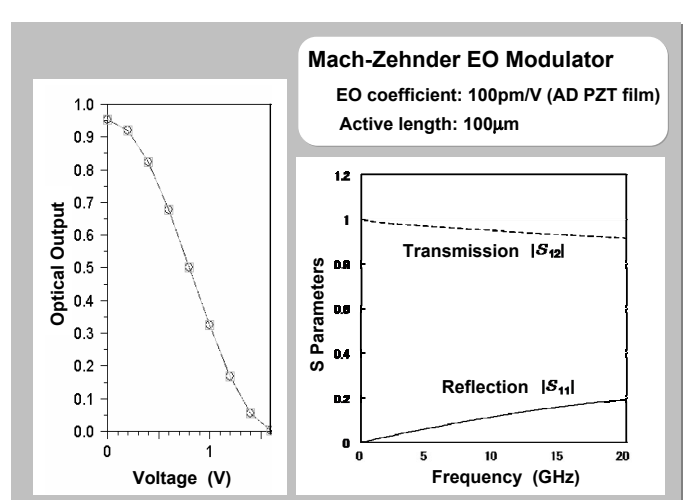


Figure 23.5.6: Simulation result of a Mach-Zehnder EO modulator.

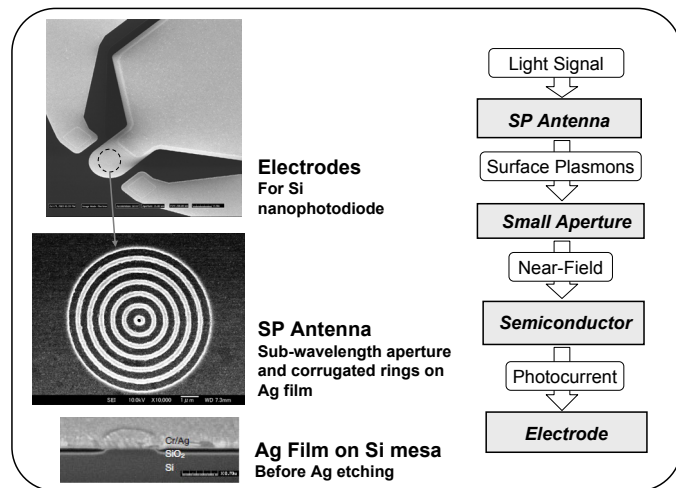


Figure 23.5.7: Structure and mechanism of Nanophotodiode.